Proceedings of the 2016 ASME Pressure Vessels & Piping Conference
SAND2016-4203C
PVP2016
July 17-21, 2016, Vancouver, British Columbia, Canada

PVP2016-63563

# COMPARISON OF INTERNAL AND EXTERNAL HYDROGEN ON FATIGUE-LIFE OF AUSTENITIC STAINLESS STEELS

**Paul J. Gibbs**
Sandia National Laboratories - CA
Livermore, CA, USA

**Chris San Marchi**
Sandia National Laboratories - CA
Livermore, CA, USA

**Kevin A. Nibur**
Hy-Performance Materials Testing, LLC.
Bend, OR, USA

**Xiaoli Tang**
Swagelok Co.
Solon, OH, USA

## ABSTRACT

The degradation of stress-controlled fatigue-life (stress-life) of notched specimens was measured in the presence of internal and in external hydrogen for two strain-hardened austenitic stainless steels: 316L and 21Cr-6Ni-9Mn. To assess the sensitivity of fatigue performance to various hydrogen conditions fatigue tests were performed in four environments: (1) in air with no added hydrogen, (2) in air after hydrogen pre-charging to saturate the steel with internal hydrogen, and in external gaseous hydrogen at pressure of (3)10 MPa (1.45 ksi), or (4) 103 MPa (15 ksi). The fatigue performance of the strain-hardened 316L and 21Cr-6Ni-9Mn steels in air was indistinguishable for the tested conditions. Decreases in the fatigue-life at a given stress level were measured in the presence of hydrogen and depended on the hydrogen environment. Testing in 103 MPa (15 ksi) external gaseous hydrogen always resulted in a clear decrease in the fatigue-life at a given maximum stress. Alloy dependent reductions in the observed life at a given maximum stress were observed in the presence of internal hydrogen or in gaseous hydrogen at a pressure of 10 MPa (1.45 ksi). The measured fatigue-life of hydrogen pre-charged specimens was comparable to the life with no intentional hydrogen additions. Accounting for the increased flow stress resulting from the supersaturation of hydrogen after pre-charging results in consistency between the measured fatigue-life of the pre-charged condition and measurements in 103 MPa (15 ksi) external hydrogen. The current results indicate that internal hydrogen may be an efficient method to infer hydrogen-assisted fatigue degradation of stainless steels in high-pressure gaseous hydrogen.

## INTRODUCTION

Austenitic stainless steels are common engineering alloys for hydrogen components due to satisfactory historical service experience and high resistance to degradation of tensile ductility in the presence of hydrogen [1]–[5]. However, relatively few austenitic stainless steels have been considered for extensive use in hydrogen pressure storage systems, with annealed 316/316L or SUS316L class steels being the most generally accepted alloy grades. While other austenitic stainless steels have demonstrated similar or superior tensile properties compared to annealed 316-based steels in gaseous hydrogen [4]–[7], manufacturers have been reluctant to use alternative steels due, in part, to the lack of hydrogen service experience and robust comparative metrics. Importantly, the decision to use 316-based austenitic stainless steels for hydrogen service often relies on quasi-static tensile property measurements, largely because these measurements are readily available, despite the fact that these data may not represent the salient failure mechanisms of in-service components.

Fatigue performance is a design-relevant metric for pressure system components subjected to repeated pressurization-depressurization cycles. Various researchers have reported hydrogen degradation of the stress-controlled fatigue-life (*i.e.* stress-life) of stainless steels using a circumferential notch [8]–[10] or microstructurally-scaled surface defect [11]–[13] and have also studied the relative impact of hydrogen on smooth fatigue specimens [7], [14], [15]. These fatigue studies often emphasize that there is a quantifiable decrease in the fatigue-life due to the presence of external gaseous hydrogen [8], [9], [11], [12]. Fatigue testing in gaseous hydrogen is challenging to execute, however, and requires specialized high-pressure testing equipment, limiting the testing to relatively few laboratories and making these tests

 

expensive. Moreover, due to the limited availability of *in situ* test facilities, long duration fatigue testing in external hydrogen is generally impractical. These considerations inhibit the ability to accurately measure the endurance limit (the stress where failure is not expected within $10^6$ fatigue cycles), an essential material parameter for stress-based designs. Test methods that do not require extensive fatigue testing in external hydrogen are beneficial if new alloys are to be considered for application in hydrogen service environments.

In some cases, the materials properties degradation by hydrogen can be probed by saturating the lattice with internal hydrogen for subsequent testing in air. In particular, austenitic stainless steels effectively retain internal hydrogen after exposure to external gaseous hydrogen at high temperature and subsequent cooling to room temperature. This technique is referred to as hydrogen pre-charging. Pre-charged specimens may then be tested in air as an analogue to testing in external gaseous hydrogen. Comparison of the tensile ductility of austenitic stainless steels (using reduction of area) show reasonable correspondence between internal and external hydrogen environmental conditions [4], [5], enabling the use of internal hydrogen to screen materials and evaluate basic trends in the tensile behavior of austenitic stainless steels. Reports of stress-life fatigue of pre-charged austenitic steels have typically reported no decrease, or a slight increase, in the stress-life in the presence of internal hydrogen [10], [13], [14]. However, to date there have been no clear comparisons made between stress-life testing with internal hydrogen versus testing in external gaseous hydrogen.

Here we compare notched stress-life fatigue of two austenitic stainless steels, 316L and 21Cr-6Ni-9Mn, with internal hydrogen and in external gaseous hydrogen. Changes in the measured fatigue-life in the various hydrogen environments are contrasted with the measured tensile stress-strain behavior to highlight the microstructural response to these different loading conditions. Hydrogen pre-charging is presented as an efficient means to screen candidate alloys for hydrogen service.

## EXPERIMENTAL METHODS

Two stainless steels were investigated, 316L and 21Cr-6Ni-9Mn (also known as XM-11); the compositions of the investigated steels are given in Table 1. Both steels were commercially produced bar supplied in a strain-hardened condition.

Specimens for the measurement of quasi-static tensile properties were machined following ASTM E-8 standard with a reduced section length of 19 mm (0.75") and a gauge diameter of 4 mm (0.16") [16]. Tension tests were performed at a constant crosshead speed of 0.02 mm/s ($8.3 \times 10^{-4}$ in. $s^{-1}$), corresponding to a nominal engineering strain rate of $1.7 \times 10^{-3}$ $s^{-1.}$ A 12.7 mm (0.5") extensometer was used to monitor the elongation of the specimen. Tension-tension fatigue specimens including a circumferential notch were also machined out of the supplied bars with nominal dimensions: major diameter of 5.7 mm (0.225"), minimum diameter of 4.06 mm (0.160"), root radius of 0.127 mm (0.005"), with an included angle of 60°. This notch corresponds to a stress concentration factor ($K_t$) of approximately 3.9 [17]. All specimens were tested in the as-machined condition with no polishing after lathe turning.

Thermal pre-charging was used to uniformly saturate some of the test specimens with internal hydrogen (referred to as the pre-charged, PC, condition). The specimens for hydrogen charging were exposed to gaseous hydrogen at pressure of 138 MPa (20 ksi) and temperature of 300 °C (572 °F) for a minimum of 10 days to achieve uniform hydrogen saturation in the specimen. Similar conditions have been summarized in detail in previous work [4], [18], and in the current testing resulted in nominally 140 weight parts per million (wt ppm.) hydrogen in the 316L and 240 wt ppm. hydrogen in the 21Cr-6Ni-9Mn alloy, measured by inert gas fusion. After thermal charging the specimens were stored at approximately -50 °C (-58 °F) to retain the hydrogen in the specimen until testing. The overall hydrogen content was verified in multiple specimens after prolonged fatigue tests and showed essentially no change.

All fatigue testing was conducted in load-control with an R-ratio of 0.1 (ratio of minimum to maximum load). All of the data presented here were collected at a temperature of 20 °C (68 °F). The nominal stresses imposed on the specimens during a test were determined from the applied load and the minimum initial cross-sectional area at the root of the notch, referred to as the net-section stress. The maximum stress during each fatigue cycle was typically limited such that the net-section stress was less than the yield stress (YS) of the tested condition (hydrogen pre-charged or non-charged respectively). The effect of stress concentration due to the notch was not explicitly considered here, though local yielding is assumed to occur near the root of the notch. Testing of the as-received (AR, *i.e.* no intentional hydrogen additions) and PC conditions was performed in laboratory air on a standard servo-hydraulic tensile test frame with the ends of the specimens threaded into pull-rods connected to spherical universal joints for alignment; no special consideration was given to specimen alignment. All testing of the PC condition was performed at 1 Hz; the AR condition tests were performed

**Table 1 - Stainless Steel Compositions**

| Alloy ID | Cr | Ni | Mn | Mo | C | N | Si | S | P |
|---|---|---|---|---|---|---|---|---|---|
| 316L | 17.54 | 12.04 | 1.15 | 2.05 | 0.020 | 0.04 | 0.51 | 0.023 | 0.028 |
| 21Cr-6Ni-9Mn | 20.45 | 6.15 | 9.55 | NR | 0.033 | 0.265 | 0.52 | 0.0013 | 0.018 |

at either 1 or 10 Hz, no significant rate dependence was apparent in the AR fatigue-life.

Tests were also conducted in external gaseous hydrogen in a minimum hydrogen pressure of either 10 MPa (1.45 ksi) at Hy-Performance Materials Testing or 103 MPa (15 ksi) at Sandia National Laboratories using dedicated servo-hydraulic test frames. Each system is outfitted with a pressure vessel to control the test environment; the test specimen is placed in the load train of the vessel and is coupled to the hydraulically driven actuation provided by the mechanical test frame. Tests in gaseous hydrogen were performed at a temperature of approximately 20 °C (68 °F) and a frequency of 1 Hz. The impurity content in the hydrogen test environment was not verified for each high-pressure test, but the purging procedure adopted (four purges with He, evacuation to sub-ambient pressures, followed by four purges with gaseous hydrogen) typically results in oxygen and water contents less than 1 and 5 parts per million by volume (vppm.), respectively [5]. The source gas was 99.9999% hydrogen. An in-line oxygen monitor in the testing system at Hy-Performance Materials Testing enabled monitoring of the oxygen content at the start and finish of every test; oxygen was maintained below 1 vppm. for all tests. Specimens were placed in self-aligning pinned joints for tests conducted in 10 MPa (1.45 ksi) hydrogen; no special consideration was given to specimen alignment during testing in 103 MPa (15 ksi) hydrogen. For the current study, runout was defined as $1.5 \times 10^6$ cycles for tests in air on the AR and PC specimens, while tests in external hydrogen were halted at $10^5$ cycles.

## RESULTS

The tensile properties of the 316L and 21Cr-6Ni-9Mn alloys studied here are summarized in Table 2. Both steels yielded continuously and displayed a relatively high YS due to the prior strain-hardening.

The 316L steel had a relatively low ultimate tensile stress (UTS) to YS ratio, typical of strain-hardened stainless steels. With the addition of internal hydrogen the yield strength of the 316L increased approximately 13 pct. with a nearly proportionate increase in the UTS, resulting in a slight decrease in the UTS to YS ratio between the PC and AR conditions. Supersaturation of hydrogen in the 316L steel had a nominal effect on the work hardening behavior during plastic deformation; a consistent increase in the work hardening rate over the entire plastic strain history was measured. Correspondingly, the uniform elongation (engineering strain at the onset of necking and plastic instability determined using the Considére criterion) of both the AR and PC conditions was approximately equal, measured as 26.6 pct. and 27.1 pct., respectively. With regard to uniaxial tensile properties, hydrogen pre-charging had the most significant impact on post-uniform deformation in the 316L steel, with a 21 pct. decrease in the reduction of area in the presence of internal hydrogen.

Trends in the tensile properties of the 21Cr-6Ni-9Mn steel show several subtle differences compared to the 316L. First, pre-charging produces a larger increase in the YS of the 21Cr-6Ni-9Mn than was measured for the 316L; the YS increased approximately 24 pct. for the PC 21Cr-6Ni-9Mn steel. The YS increase in both steels is partly due to strain-aging in the strain-hardened microstructure (approximately a 2 pct. increase in the 21Cr-6Ni-9Mn). In the 21Cr-6Ni-9Mn the increase in YS is not maintained to the UTS, and the UTS to YS ratio decreases from 1.60 in the AR condition to 1.42 in the PC condition. No increase in the work hardening rate was measured in the 21Cr-6Ni-9Mn, highlighting a change in the strain-hardening behavior due to hydrogen in this alloy compared to the 316L. The increase in yield strength in the 21Cr-6Ni-9Mn steel is only manifest in the PC condition; testing in 103 MPa (15 ksi) external gaseous hydrogen results in essentially no change in either the YS or UTS compared to the AR condition. In contrast, the uniform elongation showed a decrease from 59.5 pct. in the AR condition to 49.4 pct. and 54.0 pct. in external gaseous hydrogen and with internal hydrogen, respectively. Post-uniform elongation was more substantially reduced by the presence of internal hydrogen compared to tests in external hydrogen, likely due to the change in fracture mechanism from hydrogen-assisted surface crack propagation during testing in external hydrogen to internal crack coalescence with internal hydrogen [5].

Notched stress-life fatigue data are plotted for the 316L

**Table 2 - Stainless Steel Tensile Properties**

| Alloy ID | Condition | 0.2 pct. Offset Yield Strength (MPa) | Ultimate Tensile Strength (MPa) | UTS/YS | Uniform Elongation (pct.) | Total Elongation (pct.) | Reduction of Area (pct.) |
|---|---|---|---|---|---|---|---|
| 316L | AR | 573 | 731 | 1.28 | 26.6 | 54.5 | 76.6 |
| | PC | 648 | 793 | 1.22 | 27.1 | 47.6 | 60.2 |
| 21Cr-6Ni-9Mn | AR | 539 | 881 | 1.63 | 37.6 | 59.5 | 78.7 |
| | PC | 669 | 957 | 1.43 | 37.7 | 54.0 | 49.7 |
| | 103 MPa $H_2$ | 541 | 887 | 1.64 | 38.4 | 49.4 | 65.2 |

and 21Cr-6Ni-9Mn steels in Figure 1a and Figure 1b, respectively. Four individual conditions are plotted for each alloy, corresponding to the baseline AR condition, the PC condition, as well as testing in 10 MPa (1.45 ksi), and 103 MPa (15 ksi) external gaseous hydrogen. The stress-life data for the various conditions are plotted as the maximum imposed cyclic stress ($S_M$) as a function of cycles to failure. Also plotted in Figure 1 is a fit to the AR stress-life data where the measured cycles to failure ($N$) were fit as a function of the imposed maximum stress, presented as the Basquin equation:

Eq. 1 $$S_M = s_f N^b$$

where $s_f$ and $b$ are fitting constants. The intrinsic fatigue performance of the two alloys was statistically identical and the Basquin equation was fit to the AR data collectively for both alloys: the fit constants were 2520MPa and -0.15 for $s_f$ and $b$, respectively. The fit parameters for the various experimental conditions are given in Table 3. Also shown in Figure 1 are the 95 pct. confidence limits of the fit fatigue-life, shown by the red lines. These confidence intervals represent the relative variability in the mean life at a given stress based on the fit curve following ASTM E738 [19]. Variability in the measured failure life is systemic in fatigue data, but notched specimens typically reduce this intrinsic variability because the stress concentration localizes fatigue damage to a relatively small volume. Consistently sharp notches are difficult to machine in austenitic stainless steels, however without damaging the surface of the specimen. Observed variability in the stress-life data in Figure 1 is attributed to machining inconsistencies at the notch root, particularly for measured fatigue-lives greater than the confidence limit of the fit fatigue-life in Figure 1. However, none of these individual outliers are statistically relevant when compared to the systematic fit to the data.

The notched stress-life of 316L stainless steel decreased slightly in the presence of hydrogen, both internal and external (Figure 1a). In the case of thermally pre-charged specimens, the decrease in the stress-life is small but is frequently outside the 95 pct. confidence interval to the AR fatigue-life. In contrast, stress-life data from testing in both 10 MPa (1.45 ksi) and 103 MPa (15 ksi) external gaseous hydrogen in Figure 1a are clearly separated from the AR results. For 316L the role of varying hydrogen pressure on the maximum stress for failure at a given life appears to be negligible and the data from both hydrogen pressures overlay.

The AR and PC notched stress-life results from the 21Cr-6Ni-9Mn steel overlay in Figure 1b, and most of the PC data fall within, or are only slightly below, the confidence limits of the fit life. Similarly, tests performed in 10 MPa (1.45 ksi) external hydrogen are within the confidence interval for the AR fit, suggesting a negligible decrease in the fatigue performance for the 21Cr-6Ni-9Mn steel when exposed to 10 MPa (1.45 ksi) hydrogen at 1 Hz cycle frequencies. Of the tested conditions only the fatigue performance of the 21Cr-6Ni-9Mn tested in 103 MPa (15 ksi) external gaseous hydrogen is clearly distinguished from stress-life results of the AR condition.

## DISCUSSION

Direct comparisons between the notched stress-life of the 316L and 21Cr-6Ni-9Mn exposed to different hydrogen environments underscore that hydrogen reduced the fatigue-life of notched specimens. The measured effect of external gaseous

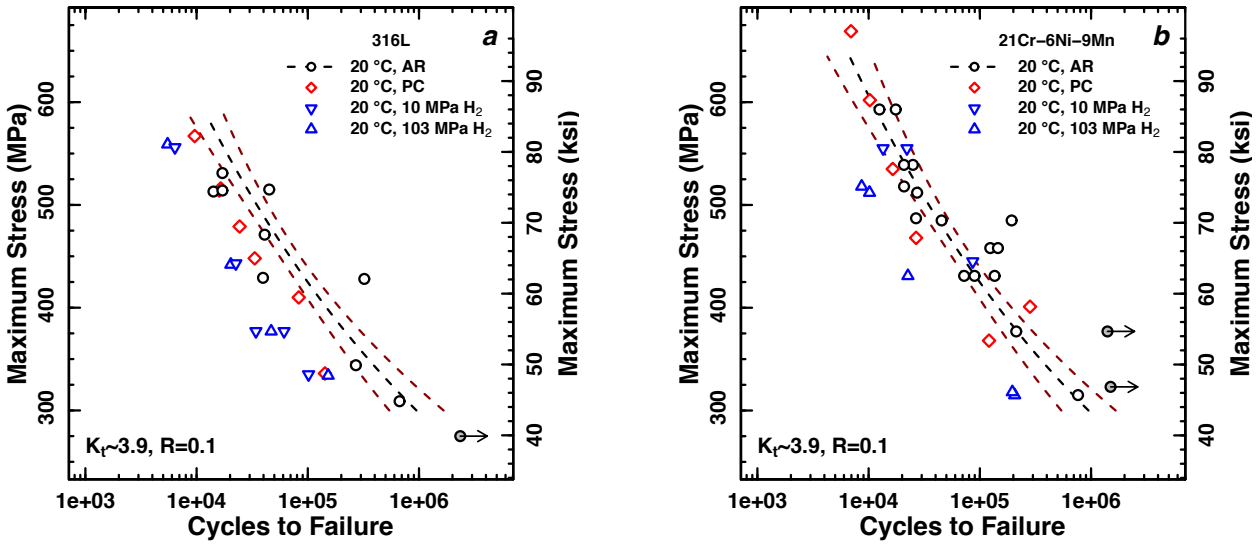


**Figure 1 Room temperature tension-tension stress-life fatigue curves plotted as a function of the maximum imposed stress of (a) 316L and (b) 21Cr-6Ni-9Mn stainless steel for four conditions: (1) as-received (AR), (2) hydrogen pre-charged (PC), as well as the AR material in (3) 10 MPa and (4) 103 MPa external gaseous hydrogen. The lines on the plots represent fits to the AR data (black) and the 95 pct. confidence interval of the fit fatigue-life (red) presented following the Basquin equation. Shaded symbols with arrows represent test conditions that did not result in failure. Notched specimens with $K_t$~3.9 [17].**

**Table 3 - Basquin Parameters**

| Alloy ID | Condition | *b-exponent* | $s_f$ (MPa) |
|---|---|---|---|
| 316L & 21Cr-6Ni-9Mn | AR | -0.15 | 2520 |
| 316L | PC | -0.18 | 3100 |
| | External $H_2$ | -0.17 | 2510 |
| 21Cr-6Ni-9Mn | PC | -0.17 | 2920 |
| | 103 MPa $H_2$ | -0.16 | 2140 |

hydrogen on the performance of 316L steel appears to be more severe than pre-charging with internal hydrogen. Alternately, for the 21Cr-6Ni-9Mn steel pre-charging and testing in 10 MPa (1.45 ksi) external hydrogen had little affect on the fatigue-life, while testing in 103 MPa (15 ksi) gaseous hydrogen reduced the fatigue-life of the steel.

The measured stress-life results must be considered in the context of how hydrogen affects the mechanical behavior of austenitic stainless steels. In particular, the tensile stress-strain behavior of the 21Cr-6Ni-9Mn showed essentially no change in the uniform deformation region in external hydrogen and negligible changes in the work hardening rate after hydrogen pre-charging while the 316L displayed only modest changes in the low strain work hardening after hydrogen pre-charging. Furthermore, the fatigue-life data in Figure 1 suggest that the underlying relationship (*i.e.* fitting the data following Eq. 1) governing the limiting life at an imposed maximum stress was unaltered by either internal or external hydrogen. The fit *b*-exponent value represents the sensitivity of the observed fatigue-life to changes in the imposed loading conditions. For both steels and the four experimentally observed environmental conditions, relatively small changes in the fit *b*-exponent values were obtained (Table 3) with the conditions in hydrogen displaying a slightly lower *b*-exponent than the fit to the as-received data. The consistency between the *b*-exponents with internal and in external hydrogen suggests similarity between these conditions and that a relationship between them should exist.

The only pronounced change in tensile properties in either steel in the presence of hydrogen was the increase in yield strength after hydrogen pre-charging. Since fatigue-life generally increases with increasing yield strength [20], it is necessary to consider the differences in the flow stress between the various hydrogen conditions when assessing the measured fatigue data. Additionally in notched specimens, the extent of the local plasticity adjacent to the notch, which is presumed to govern the fatigue-life [21]–[25], will be determined by the ratio of the maximum applied stress to the material yield stress, as well as the notch geometry.

In order to account for the local stress environment in a given fatigue test, the measured fatigue data can be replotted normalizing the maximum stress by the hydrogen dependent yield strength (*i.e.* $S_M$/YS). The measured stress-life data are plotted using the yield strength normalized maximum stress as the ordinate axis in Figure 2a and Figure 2b for the 316L and 21Cr-6Ni-9Mn, respectively. The macroscopic YS was assumed to be unaffected by external hydrogen based on previous experimental studies [4], [5] as well as the YS data in Table 2. The measured YS for the pre-charged condition

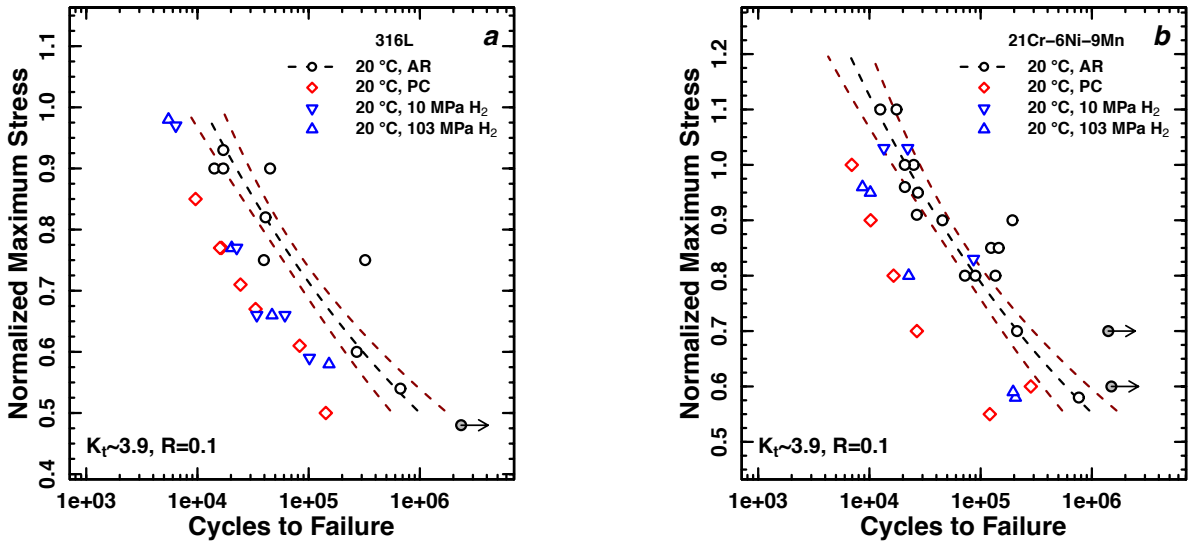


**Figure 2 Room temperature tension-tension stress-life fatigue curves plotted as a function of the maximum imposed stress normalized by the hydrogen-dependent yield strength of (a) 316L and (b) 21Cr-6Ni-9Mn stainless steel for four conditions: (1) as-received (AR), (2) hydrogen pre-charged (PC), as well as the AR material in (3) 10 MPa and (4) 103 MPa external gaseous hydrogen. The lines on the plots represent fits to the AR data (black) and the 95 pct. confidence interval of the fit fatigue-life (red) presented following the Basquin equation. Shaded symbols with arrows represent test conditions that did not result in failure. Notched specimens with $K_t$~3.9 [17].**

(Table 2) was used to normalize the fatigue data measured from pre-charged samples. The regression lines in Figure 2 are the same fits as were plotted in Figure 1 but are scaled to the appropriate YS from Table 2 for 316L and 21Cr-6Ni-9Mn respectively.

In 316L, accounting for the increase in YS due to hydrogen pre-charging aligns the results from pre-charged specimens with the results from testing in external hydrogen, all three data sets with hydrogen clearly occupy a single band below the lower bound confidence limit of the average life of the as-received condition. Likewise, accounting for the condition dependent YS of 21Cr-6Ni-9Mn stainless steel aligns the PC results with the tests in 103 MPa (15 ksi) external hydrogen; these two conditions represent the lower-bound fatigue-life in Figure 2b.

While the data in Figure 2b clearly show a decrease in the fatigue-life of 21Cr-6Ni-9Mn in the hydrogen pre-charged condition and in 103 MPa (15 ksi) external hydrogen, the relatively limited data in gaseous hydrogen at 10 MPa (1.45 ksi) are within the confidence interval of the as-received fatigue-life. There are several possible explanations for the difference in stress-life performance between the investigated alloys as a function of gas pressure. The dissimilarity in the pressure sensitivity may arise from changes in the hydrogen-surface interactions between the two alloys. Hydrogen ingress may be may be more sensitive to pressure in 21Cr-6Ni-9Mn compared to 316L, resulting in greater sensitivity to external hydrogen pressure. Alternatively, strain-assisted martensite formation in 316L stainless steels has been suggested to act as a rapid pathway for hydrogen transport [26], [27] and has also been observed to display a synergistic interaction with hydrogen adjacent to fatigue cracks [13], [15], [26], [28], [29]. In contrast, the 21Cr-6Ni-9Mn does not form strain-induced alpha prime martensite, eliminating this microstructural feature related to observed hydrogen interactions. Changes in long-range transport, local crack environment, or hydrogen ingress may result in changes in the sensitivity to external hydrogen pressure. Additional testing is required to clarify the role of hydrogen pressure on the stress-life in austenitic steels.

Having established analogies between the limiting fatigue behavior with internal and in external hydrogen, it is informative to directly compare the relative environmentally assisted degradation of the fatigue strength between the investigated alloys. One means to compare alloys is to calculate a safety factor multiplier (SFM) as suggested in the CHMC1-2014 standard [30]. This standard predicates that the effects of hydrogen on fatigue can be incorporated into existing design factors by calculating relative fatigue performance as a multiplier to the nominal safety factor of a component (*e.g.* the SFM). The SFM is determined by the maximum value of either the ratio of the imposed fatigue stress in air to a relevant hydrogen environment at various fatigue lifetimes between $10^3$ and $10^5$ cycles or the ratio of notched tensile strength in air and in hydrogen (notched tensile tests are not considered here).

Figure 3 shows the calculated safety factor multiplier for both steels in external hydrogen (solid lines) and with internal hydrogen (dashed lines) incorporating the adjustment for increased yield strength after pre-charging. The horizontal dash-dot line indicates a SFM of unity where no hydrogen effect is measured. Safety factor multiplier values greater than one indicate a decrease in the fatigue performance due to hydrogen. For both the 316L and the 21Cr-6Ni-9Mn, the SFM increases with increasing fatigue-life. In external gaseous hydrogen this results in the largest decrease in fatigue-life due to the presence of hydrogen at the lowest maximum stresses where failure was observed, *i.e.* maximum fatigue stresses of approximately 300 MPa (43.5 ksi) in the 21Cr-6Ni-9Mn and 330 MPa (47.8 ksi) in the 316L steel. The maximum SFM for the 316L is approximately 1.40 and there is no significant difference between the hydrogen pre-charged data and tests in external hydrogen. Conversely, in the 21Cr-6Ni-9Mn, the SFM for the hydrogen pre-charged data and testing in external hydrogen are separated at high fatigue-lives, with the SFM calculated based on internal hydrogen resulting in the maximum SFM of approximately 1.35 compared to 1.23 for testing in external hydrogen. However, this difference is likely a byproduct of scatter in the data near the endurance limit in the 21Cr-6Ni-9Mn alloy and the relatively limited number of tests in gaseous hydrogen. Overall the magnitude of the SFM for 21Cr-6Ni-9Mn stainless steel is similar to the 316L stainless steel.

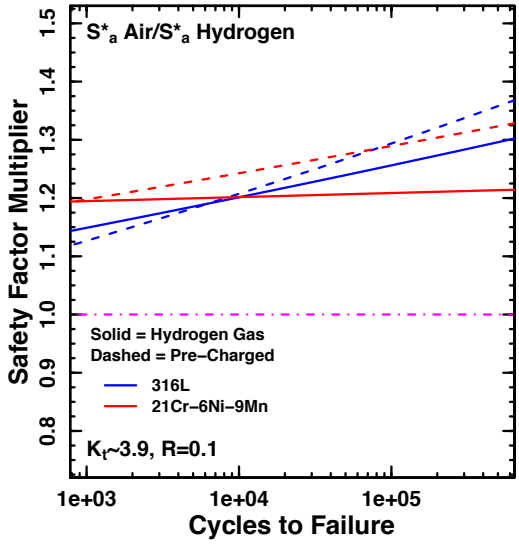


**Figure 3 Room temperature safety factor multiplier curves for 316L and 21Cr-6Ni-9Mn stainless steel tested with internal and external hydrogen. Calculation of safety factor multiplier based on normalized fatigue-life for both conditions. Hydrogen pressure for 21Cr-6Ni-9Mn was 103 MPa, 316L data are from 10 MPa and 103 MPa external gaseous hydrogen**

Most important, measurement of the fatigue-life at low imposed stress amplitudes around near 'infinite' life for the AR condition, showed the largest decrease in allowable stress at a

given life due to the presence of hydrogen. Low stress amplitude conditions, resulting in long fatigue lives, also represent the most challenging and costly tests to perform in external hydrogen. The reasonable coincidence of the stress-life curves between the various hydrogen environments when normalized as in Figure 2 suggests that hydrogen pre-charged specimens provide a method to efficiently identify the fatigue performance of austenitic stainless steels in the presence of hydrogen. Focused experiments in external hydrogen could then be effectively employed to ensure material reliability. However, it is important to emphasize that no mechanistic basis for adjustment of the fatigue life curves based on the hydrogen-condition dependent yield strength has been developed, and there are likely subtle changes in the fatigue crack initiation life, fatigue crack growth life, and crack propagation behaviors between testing with internal *versus* in external hydrogen that should be explored further.

## SUMMARY

The stress-controlled fatigue life of circumferentially notched specimens of 316L and 21Cr-6Ni-9Mn austenitic stainless steels were compared for four environments: (1) in the as-received condition, (2) after hydrogen pre-charging, in external gaseous hydrogen at pressure of (3) 10 MPa (1.45 ksi) and (4) 103 MPa (15 ksi). The following observations can be made:

1) The fatigue performance of the as-received (*i.e.* no intentional hydrogen additions) 316L and 21Cr-6Ni-9Mn steels in air were indistinguishable.
2) The fatigue-life of 316L was reduced by the presence of both internal and external hydrogen. The decrease in life was essentially independent of pressure in the range of 10 MPa (1.45 ksi) to 103 MPa (15 ksi), while hydrogen pre-charging resulted in a smaller absolute decrease in the fatigue-life.
3) The fatigue-life of 21Cr-6Ni-9Mn stainless steel was only reduced during testing in 103 MPa (15 ksi) external hydrogen; tests performed in 10 MPa (1.45 ksi) and after thermal pre-charging were within the 95 pct. confidence interval of the average fatigue-life with no added hydrogen.
4) Normalization of the maximum cyclic stresses by the yield strength accounted for the effects of pre-charging on the stress-life data. This normalization resulted in convergence between the measured stress-life behavior in 103 MPa (15 ksi) external hydrogen and with internal hydrogen; these data appear to represent the lower-bound room temperature fatigue behavior for testing at 1 hz. Fatigue testing of thermally pre-charged specimens then appears to be a viable means to efficiently screen the fatigue performance of candidate alloys for hydrogen service.
5) Comparisons of environmentally-assisted degradation of fatigue-life of 316L and 21Cr-6Ni-9Mn steels suggests that they are similarly affected by hydrogen, with a calculated maximum safety factor multiplier of 1.4 and 1.35 for the two alloys, respectively.

## ACKNOWLEDGMENTS

The authors gratefully acknowledge assistance from J.A. Campbell for hydrogen pressure systems support. We also acknowledge funding support by the U.S. Department of Energy Fuel Cell Technologies Office through the Hydrogen Storage program element under project ST113. Sandia National Laboratories is a multi-program laboratory managed and operated by Sandia Corporation, a wholly owned subsidiary of Lockheed Martin Corporation, for the U.S. Department of Energy's National Nuclear Security Administration under contract DE-AC04-94AL85000.


## REFERENCES

[1] M. B. Whiteman and A. R. Troiano, "Hydrogen embrittlement of austenitic stainless steel," *Corrosion*, vol. 21, no. 2, pp. 53–56, 1965.

[2] R. M. Vennett and G. S. Ansell, "The effect of high-pressure hydrogen upon the tensile properties and fracture behavior of 304 L stainless steel," *ASM Trans. Q.*, vol. 20, no. 2, pp. 242–251, 1967.

[3] M. L. Holzworth, "Hydrogen embrittlement of type 304L stainless steel," *Corrosion*, vol. 25, no. 3, pp. 107–115, 1969.

[4] C. San Marchi, D. K. Balch, K. Nibur, and B. P. Somerday, "Effect of High-Pressure Hydrogen Gas on Fracture of Austenitic Steels," *J. Press. Vessel Technol.*, vol. 130, no. 041401, pp. 1–9, 2008.

[5] C. San Marchi, T. Michler, K. A. Nibur, and B. P. Somerday, "On the physical differences between tensile testing of type 304 and 316 austenitic stainless steels with internal hydrogen and in external hydrogen," *Int. J. Hydrogen Energy*, vol. 35, no. 18, pp. 9736–9745, 2010.

[6] T. Michler, K. Berreth, J. Naumann, and E. Sattler, "Analysis of martensitic transformation in 304 type stainless steels tensile tested in high pressure hydrogen

 

atmosphere by means of XRD and magnetic induction," *Int. J. Hydrogen Energy*, vol. 37, pp. 3567–3572, 2012.

[7] S. Matsuoka, J. Yamabe, and H. Matsunaga, "Criteria for determining hydrogen compatibility and the mechanisms for hydrogen-assisted, surface crack growth in austenitic stainless steels," *Eng. Fract. Mech.*, vol. 153, pp. 103–127, 2016.

[8] T. Michler, J. Naumann, and E. Sattler, "Influence of high pressure gaseous hydrogen on S–N fatigue in two austenitic stainless steels," *Int. J. Fatigue*, vol. 51, pp. 1–7, 2013.

[9] T. Michler, J. Naumann, S. Weber, M. Martin, and R. Pargeter, "S-N fatigue properties of a stable high-aluminum austenitic stainless steel for hydrogen applications," *Int. J. Hydrogen Energy*, vol. 38, pp. 9935–9941, 2013.

[10] C. San Marchi, B. P. Somerday, and K. A. Nibur, "Fatigue crack initiation in hydrogen-precharged austenitic stainless steel," in Hydrogen-Materials Interactions, Proceedings of the *2012 International Hydrogen Conference*, 2014, pp. 365–373.

[11] Y. Murakami, T. Kanezaki, Y. Mine, and S. Matsuoka, "Hydrogen Embrittlement Mechanism in Fatigue of Austenitic Stainless Steels," *Metall. Mater. Trans. A*, vol. 39, pp. 1327–1339, 2008.

[12] T. Kanezaki, C. Narazaki, Y. Mine, S. Matsuoka, and Y. Murakami, "Effects of hydrogen on fatigue crack growth behavior of austenitic stainless steels," *Int. J. Hydrogen Energy*, vol. 33, pp. 2604–2619, 2008.

[13] Y. Murakami, T. Kanezaki, and Y. Mine, "Hydrogen Effect against Hydrogen Embrittlement," *Metall. Mater. Trans.*, vol. 41A, pp. 2548–2562, 2010.

[14] D. M. Matson, A. Saigal, and C. San Marchi, "Fatigue behavior of austenitic stainless steel alloys thermall pre-charged in gaseous hydrogen," in Hydrogen-Materials Interactions, Proceedings of the *2012 International Hydrogen Conference*, 2014, pp. 375–382.

[15] G. Schuster and C. Altstetter, "Fatigue of Stainless Steel in Hydrogen," *Metall. Trans. A*, vol. 14, pp. 2085–2090, 1983.

[16] "ASTM E8/E8M - 13a Standard Test Methods for Tension Tesing of Metallic Materials." ASTM International, West Conshohocken, PA, p. 28, 2013.

[17] N. Noda and Y. Takase, "Stress concentration formula useful for all notch shape in a round bar (comparison between torsion, tension and bending)," *Int. J. Fatigue*, vol. 28, pp. 151–163, 2006.

[18] C. San Marchi, B. P. Somerday, X. Tang, and G. H. Schiroky, "Effects of alloy composition and strain hardening on tensile fracture of hydrogen-precharged type 316 stainless steels," *Int. J. Hydrogen Energy*, vol. 33, pp. 889–904, 2008.

[19] "ASTM E739 - 10 Standard Practice for Statistical Analysis of Linear or Linearized Stress-Life (S-N) and Strain-Life (e-N) Fatigue Data." ASTM International, West Conshohocken, PA, p. 7, 2010.

[20] G. E. Dieter, *Mechanical Metallurgy*, Third. Boston, MA: McGraw Hil, 1986, p. 419.

[21] K. Saanouni and C. Bathias, "Study of fatigue crack initiation in the vicinity of notches," vol. 16, no. 5, pp. 695–706, 1982.

[22] B. F. Langer, "Design of Pressure Vessels for Low-Cycle Fatigue," *J. Basic Eng.*, vol. 84, no. 3, pp. 389–399, 1962.

[23] C. E. Jaske and W. J. O'Donnell, "Fatigue Design Criteria for Pressure Vessel Alloys," *J. Press. Vessel Technol.*, vol. 99, no. 4, pp. 584–592, 1977.

[24] J. Colin and A. Fatemi, "Variable amplitude cyclic deformation and fatigue behaviour of stainless steel 304L including step, periodic, and random loadings," *Fatigue Fract. Eng. Mater. Struct.*, vol. 33, pp. 205–220, 2010.

[25] M. Kamaya and M. Kawakubo, "Mean stress effect on fatigue strength of stainless steel," *Int. J. Fatigue*, vol. 74, pp. 20–29, 2015.

[26] G. Han, J. He, S. Fukuyama, and K. Yokogawa, "Effect of strain-induced martenite on hydrogen embrittlement of sensatized austenitic stainless steels at low temperatures," *Acta Mater.*, vol. 46, no. 13, pp. 4559–4570, 1998.

[27] M. Martin, S. Weber, W. Theisen, T. Michler, and J. Naumann, "Effect of alloying elements on hydrogen environment embrittlement of AISI type 304 austenitic stainless steel," *Int. J. Hydrogen Energy*, vol. 36, pp. 15888–15898, 2011.

[28] S. Fukuyama, K. Yokogawa, K. Kudo, and M. Araki, "Fatigue Properties of Type 304 Stainless Steel in High Pressure Hydrogen at Room Temperature," *Trans. Japan Inst. Met.*, vol. 26, no. 5, pp. 325–331, 1985.

[29] M. L. Martin, P. Sofronis, I. M. Robertson, T. Awane, and Y. Murakami, "A microstructural based understanding of hydrogen-enhanced fatigue of stainless steels," *Int. J. Fatigue*, vol. 57, pp. 28–36, 2013.

[30] "ANSI/CSA CHMC 1-2014: Test methods for evaluating material compatibility in compressed hydrogen applications - metals." CSA Group, Ontario, Canada, p. 46, 2014.

 